Mon. Not. R. Astron. Soc. **378,** 881–887 (2007) doi:10.1111/j.1365-2966.2007.11767.x

Broad-band optical polarimetric study of IC 1805

Biman J. Medhi,[1⋆] G. Maheswar,[1] K. Brijesh,[1] J. C. Pandey,[2] T. S. Kumar[1] and R. Sagar[1]

[1]*Aryabhatta Research Institute of Observational Sciences, Manora Peak, Nainital 263129, India*
[2]*Tata Institute of Fundamental Research, Homi Bhabha Road, Mumbai 400005, India*

Accepted 2007 March 21. Received 2007 March 15; in original form 2007 February 3

ABSTRACT

We present the *BVR* broad-band polarimetric observations of 51 stars belonging to the young open cluster IC 1805. Along with the photometric data from the literature, we have modelled and subtracted the foreground dust contribution from the maximum polarization ($P_{\rm max}$) and colour excess [E ($B - V$)]. The mean value of the $P_{\rm max}$ for intracluster medium and the foreground are found to be 5.008 ± 0.005 and 4.865 ± 0.022 per cent, respectively. Moreover, the mean value of the wavelength of maximum polarization ($\lambda_{\rm max}$) for intracluster medium is 0.541 ± 0.003 m, which is quite similar as the general interstellar medium (ISM). The resulting intracluster dust component is found to have negligible polarization efficiency as compared to interstellar dust. Some of the observed stars in IC 1805 have shown the indication of intrinsic polarization in their measurements.

Key words: polarization – dust, extinction – open clusters and associations: individual: IC 1805.

1 INTRODUCTION

Polarization of starlight is one among a number of properties manifested by interstellar dust grains. Wavelength dependence of polarization, for instance, can give information on the size distribution of grains towards different Galactic directions. Polarization is thought to be caused by the same dust grain responsible for the reddening of starlight. According to the Davis & Greenstein mechanism (Davis & Greenstein 1951), the polarization of starlight is caused by the selective extinction due to the elongated dust grains aligned in space possibly due to magnetic field.

In order to investigate the distribution and characteristic of dust grains, we have selected the young open cluster IC 1805. The reddening law is anomalous in this direction and the extinction is non-uniform over the cluster region (Borgman 1961; Johnson 1968; Ishida 1969; Turner 1976; Sagar 1987). The polarimetric components produced by the Galactic dust located in front of the cluster can be found out from maximum polarization $P_{\rm max}$ and colour excess E ($B - V$) (Marraco, Vega & Vrba 1993). By removing the effect of dust located on the line of sight from the data, one can study the component associated with the internal extinction of the cluster. The young and rich open cluster IC 1805[RA (J2000) : $02^{\rm h}32^{\rm m}42^{\rm s}$, Dec.(J2000) : $+61^{\circ}27'00''$] is the core of the CasOB6 association. It is located in the Perseus spiral arm, radially outwards from the local spiral arm. IC 1805 is situated in a H II region and embedded in W4 molecular cloud. The colour excess E ($B - V$) for the cluster members varies from 0.52 to 1.3 mag (Joshi & Sagar 1983). From the near-infrared study of IC 1805, Sagar & Yu (1990) found that the distribution of dust and patchy ionized gas appear to be the cause of non-uniform extinction across the cluster face. The relative proper-motion cluster membership study was done by Vasilevskis, Sanders & van Altena (1965) in a field of about 0.66 deg^2, centred on the O-type giant VSA 148 for 350 stars with a mean error of $\pm$0.16 arcsec per century. Sanders (1972) revised these membership probabilities by applying the maximum-likelihood method. The recent estimation of cluster distance is $\simeq$2.4 kpc (Joshi & Sagar 1983), though the earlier estimate varies from 1.6 to 2.5 kpc.

The previous polarimetric study on IC 1805 was carried out by Guetter & Vrba (1989), for 24 member stars brighter than visual magnitude of $\simeq$12 mag. In order to study details about the grain alignment and particle size distribution, we have observed 32 member stars (nine star common with Guetter & Vrba 1989) brighter than visual magnitude of $\simeq$15.5 mag in IC 1805. The next section describes the details of instrumentation, observation and data reduction, while the main results are given and discussed in the remaining part of the paper.

2 INSTRUMENTATION AND OBSERVATION

The ARIES Imaging Polarimeter (AIMPOL) consists of a half-wave plate (HWP) modulator and a beam-splitting Wollaston prism analyser placed in the telescope beam path to produce ordinary and extraordinary images in slightly different directions separated by about 27 pixel.

⋆E-mail: biman@aries.ernet.in

A focal reducer (85 mm, f/1.8) is placed between Wollaston prism and CCD camera. The detail descriptions about the AIMPOL are available in Rautela, Joshi & Pandey (2004) (also see Ramaprakash et al. 1998).

By definition, the ratio $R(\alpha)$ is given by

$$R(\alpha) = \frac{I_o/I_e - 1}{I_o/I_e + 1} = P\cos(2\theta - 4\alpha) \quad (1)$$

which is the difference between the intensities of the ordinary (I_o) and extraordinary (I_e) beams to their sum, P is the fraction of the total light in the linearly polarized condition and θ is the position angle of plane of polarization. It is denoted by normalized Stokes' parameter $q(= Q/I)$, when the HWP's fast axis is aligned to the reference axis ($\alpha = 0^\circ$). Similarly, the normalized Stokes' parameter $u(= U/I), q_1(= Q_1/I), u_1(= U_1/I)$ are also the ratios $R(\alpha)$, when the HWP are at 22.5°, 45° and 67.5°, respectively. In principle, P and θ can be determined by using only two Stokes' parameters q and u. In reality, the situation is not so simple because of two reasons: (i) the responsivity of the system to the two orthogonal polarization components may not be same and (ii) the responsivity of the CCD is a function of position on its surface. Therefore, the signals which are actually measured in the two images (I'_o and I'_e) may differ from the observed one by the following formula (Ramaprakash et al. 1998):

$$\frac{I'_o(\alpha)}{I'_e(\alpha)} = \frac{I_o(\alpha)}{I_e(\alpha)} \times \frac{F_o}{F_e}, \quad (2)$$

and equation (1) can be rewritten as

$$R(\alpha) = \frac{(I_o/I_e \times F_o/F_e) - 1}{(I_o/I_e \times F_o/F_e) + 1} = P\cos(2\theta - 4\alpha), \quad (3)$$

where F_o and F_e represent the effects mentioned above and the ratio is given by

$$\frac{F_o}{F_e} = \left[\frac{I'_o(0^\circ)}{I'_e(45^\circ)} \times \frac{I'_o(45^\circ)}{I'_e(0^\circ)} \times \frac{I'_o(22.5^\circ)}{I'_e(67.5^\circ)} \times \frac{I'_o(67.5^\circ)}{I'_e(22.5^\circ)}\right]^{1/4}. \quad (4)$$

Substituting the ratio in equation (3) and fitting the cosine curve to the four values of $R(\alpha)$, the values of P and θ could be obtained. The individual errors associated with the four values of $R(\alpha)$ putting as a weight while calculating P, θ and their respective errors.

The optical imaging polarimetry of the two fields A and B (see Fig. 1) in IC 1805 was carried out to study the contribution of interstellar and intracluster material on linear polarization. The data were obtained on 2006 October 12 and 13 using the TK 1024 × 1024 pixel^2 CCD camera mounted on the Cassegrain focus of the 104-cm Sampurnanand Telescope of ARIES, Nainital in B, V and R ($\lambda_{B_{\rm eff}} = 0.440\,\mu$m, $\lambda_{V_{\rm eff}} = 0.550\,\mu$m and $\lambda_{R_{\rm eff}} = 0.660\,\mu$m) photometric bands. Each pixel of the CCD corresponds to 1.73 arcsec and the field of view is ∼8 arcmin diameter on the sky. The FWHM (full width at half-maximum) of the stellar image varies from 2 to 3 pixel. The readout noise and gain of the CCD are 7.0 e^- and 11.98 e^-/ADU, respectively. The fluxes for all of our programme stars were extracted by aperture photometry after the bias subtraction in the standard manner using IRAF. Instead of a robust flat-fielding technique, we are using equation (3) to make uniform response, as mentioned above.

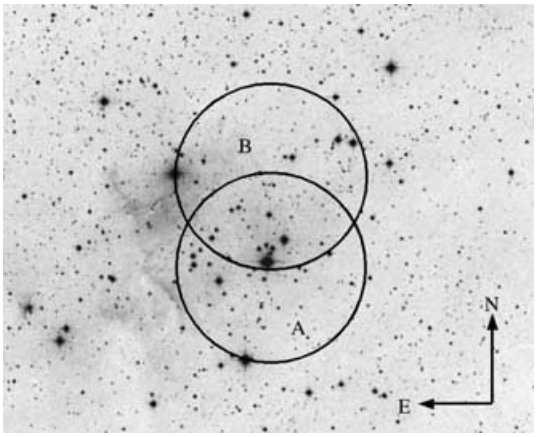

Figure 1. The 18.00 × 21.00 arcmin^2 B-band image of the fields A & B of IC 1805, reproduced from the Digitized Sky Survey.

Standard stars for null polarization and for the zero-point of the polarization position angle were taken from Schmidt, Elston & Lupie (1992). The results for polarized standards are given in Table 1. From the results, we can conclude that the observed polarization and position angles are matching with Schmidt et al. (1992) within the error limit. The average value of instrumental polarization is found to be about ∼0.04 per cent.

The AIMPOL does not have a grid placed to avoid the overlapping of ordinary image with the extraordinary image of an adjacent region 27 pixels away from it. In the care of target sources, we have selected (usually) only those which are well isolated. However, due to the overlapping, sky at a region gets doubled. However, we found the sky variation at different locations not to be very significant. Therefore, the effect gets cancelled when we consider both ordinary and extraordinary images of these target sources for the analysis.

Table 1. Observed polarized standard stars.

Star name	Filter	$P \pm \epsilon_P$(per cent)	$\theta \pm \epsilon_\theta(^\circ)$	$P \pm \epsilon_P$(per cent)	$\theta \pm \epsilon_\theta(^\circ)$
		Published data		This paper	
Hiltner-960	*B*	5.72 ± 0.06	55.06 ± 0.31	5.60 ± 0.21	54.62 ± 1.08
	V	5.66 ± 0.02	54.79 ± 0.11	5.71 ± 0.15	53.32 ± 0.05
	R	5.21 ± 0.03	54.54 ± 0.16	5.19 ± 0.06	54.81 ± 0.34
HD204827	*B*	5.65 ± 0.02	58.20 ± 0.11	5.75 ± 0.09	58.63 ± 0.45
	V	5.32 ± 0.02	58.73 ± 0.08	5.36 ± 0.03	60.19 ± 0.17
	R	4.89 ± 0.03	59.10 ± 0.17	4.90 ± 0.23	58.82 ± 1.14
BD+64°106	*B*	5.51 ± 0.09	97.15 ± 0.47	5.44 ± 0.10	99.42 ± 0.51
	V	5.69 ± 0.04	96.63 ± 0.18	5.49 ± 0.13	97.06 ± 0.17
	R	5.15 ± 0.10	96.74 ± 0.54	5.21 ± 0.02	97.38 ± 0.11
HD19820	*B*	4.70 ± 0.04	115.70 ± 0.22	4.84 ± 0.23	113.42 ± 0.11
	V	4.79 ± 0.03	114.93 ± 0.17	4.92 ± 0.11	114.50 ± 0.11
	R	4.53 ± 0.03	114.46 ± 0.17	4.73 ± 0.14	113.82 ± 0.28

Table 2. Observed *BVR* polarization values for different stars in IC 1805.

Id	M_V (mag)	$P_B \pm \epsilon_p$(per cent)	$\theta_B \pm \epsilon_\theta(^\circ)$	$P_V \pm \epsilon_p$(per cent)	$\theta_V \pm \epsilon_\theta(^\circ)$	$P_R \pm \epsilon_p$(per cent)	$\theta_R \pm \epsilon_\theta(^\circ)$
112[a]	09.91	6.42 ± 0.09	121.3 ± 0.4	6.80 ± 0.09	121.1 ± 0.1	6.40 ± 0.14	120.7 ± 0.6
118[a]	10.30	5.89 ± 0.15	122.8 ± 0.2	5.90 ± 0.01	121.5 ± 0.1	5.79 ± 0.01	121.3 ± 0.6
121	11.59	6.20 ± 0.18	126.8 ± 0.7	6.35 ± 0.09	126.7 ± 0.3	5.96 ± 0.09	126.4 ± 0.4
122	13.73	4.99 ± 0.61	120.6 ± 3.6	5.10 ± 0.51	118.5 ± 0.1	5.04 ± 0.43	118.6 ± 2.4
123	13.88	2.90 ± 0.14	121.6 ± 1.4	3.84 ± 0.18	120.2 ± 1.3	3.05 ± 0.15	121.6 ± 0.3
128	13.40	3.41 ± 0.12	108.7 ± 0.8	3.92 ± 0.17	120.0 ± 1.0	3.80 ± 0.09	118.8 ± 0.6
129	14.06	5.07 ± 0.18	123.4 ± 1.3	5.78 ± 0.14	126.2 ± 1.2	5.21 ± 0.18	124.5 ± 1.4
130[b]	13.26	4.75 ± 0.30	124.0 ± 0.5	5.53 ± 0.03	124.5 ± 1.0	5.15 ± 0.04	126.5 ± 0.1
133[b]	13.56	3.28 ± 0.38	118.3 ± 3.3	3.64 ± 0.19	125.9 ± 1.5	3.30 ± 0.48	123.4 ± 4.1
136[a]	11.04	5.39 ± 0.10	121.9 ± 0.5	5.41 ± 0.09	119.9 ± 0.4	5.38 ± 0.04	120.9 ± 0.2
138[a]	09.58	5.80 ± 0.08	122.9 ± 0.4	6.31 ± 0.08	119.0 ± 0.3	5.40 ± 0.36	120.0 ± 2.3
139	13.10	5.12 ± 0.04	123.1 ± 0.2	5.30 ± 0.17	119.3 ± 0.8	5.10 ± 0.07	121.0 ± 0.4
143	11.40	4.68 ± 0.04	125.4 ± 0.2	5.25 ± 0.05	122.5 ± 0.2	4.80 ± 0.07	122.6 ± 0.4
146[b]	13.53	5.44 ± 0.56	124.7 ± 2.9	5.72 ± 0.34	117.3 ± 1.7	4.97 ± 0.07	119.4 ± 0.4
147	13.34	4.23 ± 0.30	122.6 ± 3.2	4.86 ± 0.15	122.1 ± 0.8	4.71 ± 0.17	122.2 ± 0.9
149[a]	11.24	4.37 ± 0.09	122.4 ± 0.5	4.93 ± 0.09	119.6 ± 0.5	4.56 ± 0.05	118.3 ± 0.3
154	14.07	4.19 ± 0.59	114.7 ± 3.8	4.27 ± 0.23	115.6 ± 1.5	4.07 ± 0.25	123.8 ± 1.8
155[b]	14.39	4.95 ± 0.66	111.5 ± 3.8	4.52 ± 0.17	116.6 ± 1.0	4.35 ± 0.09	111.3 ± 0.6
156[a]	12.03	4.19 ± 0.05	122.2 ± 0.3	4.28 ± 0.04	120.6 ± 0.2	3.55 ± 0.17	122.6 ± 1.3
157	13.48	5.17 ± 0.29	121.4 ± 1.2	5.67 ± 0.30	119.8 ± 1.5	5.54 ± 0.05	120.8 ± 0.2
158	12.73	3.98 ± 0.11	122.9 ± 4.4	4.50 ± 0.10	126.1 ± 0.6	4.27 ± 0.02	127.5 ± 0.1
160[a]	08.11	5.58 ± 0.19	117.4 ± 0.9	5.91 ± 0.46	117.5 ± 2.2	5.30 ± 0.06	117.4 ± 0.3
162	12.55	5.63 ± 0.46	121.9 ± 2.3	5.77 ± 0.08	118.3 ± 0.4	5.57 ± 0.22	119.5 ± 1.2
165	12.77	5.23 ± 0.14	122.4 ± 0.7	5.68 ± 0.16	119.0 ± 0.8	5.18 ± 0.04	119.3 ± 0.2
166	11.97	4.74 ± 0.31	119.6 ± 1.3	4.99 ± 0.29	119.2 ± 0.2	4.49 ± 0.14	120.5 ± 0.2
168	13.72	6.06 ± 0.82	122.0 ± 0.8	5.29 ± 0.34	117.1 ± 1.8	5.16 ± 0.10	119.3 ± 0.5
170	10.07	3.52 ± 0.09	121.2 ± 0.1	3.75 ± 0.07	118.3 ± 0.5	3.44 ± 0.26	118.8 ± 2.1
171	13.13	5.16 ± 0.13	124.0 ± 0.6	5.24 ± 0.14	115.4 ± 2.0	5.13 ± 0.05	119.5 ± 0.3
173[b]	13.81	2.67 ± 0.12	112.3 ± 1.2	2.62 ± 0.09	116.0 ± 1.0	2.59 ± 0.09	118.8 ± 0.1
174	11.63	5.29 ± 0.17	119.5 ± 0.8	5.27 ± 0.01	118.3 ± 0.1	5.06 ± 0.02	117.9 ± 0.1
175	13.10	4.68 ± 0.44	114.4 ± 2.5	4.96 ± 0.24	115.1 ± 1.3	4.48 ± 0.14	116.1 ± 0.8
182	13.38	5.61 ± 0.05	117.0 ± 0.1	5.94 ± 0.09	122.9 ± 1.0	5.53 ± 0.02	121.1 ± 0.2
183[a]	11.15	5.19 ± 0.37	121.0 ± 2.0	5.01 ± 0.04	118.5 ± 0.2	4.89 ± 0.06	118.5 ± 0.3
184[b]	13.64	4.20 ± 0.28	120.4 ± 1.6	3.82 ± 0.11	120.0 ± 0.7	3.81 ± 0.16	124.6 ± 1.2
185[b]	11.58	5.56 ± 0.05	121.9 ± 0.2	5.44 ± 0.19	120.1 ± 0.9	4.99 ± 0.07	120.2 ± 0.3
188	12.68	4.90 ± 0.12	122.8 ± 0.8	5.38 ± 0.09	121.2 ± 0.4	4.76 ± 0.18	118.1 ± 0.4
191	12.96	3.99 ± 0.11	113.0 ± 1.0	4.32 ± 0.18	105.8 ± 6.4	3.97 ± 0.09	117.5 ± 0.7
192[a]	08.43	3.38 ± 0.16	123.0 ± 1.0	3.52 ± 0.11	115.0 ± 0.8	3.31 ± 0.18	118.4 ± 1.6
354[b]	13.43	4.75 ± 0.35	125.9 ± 1.7	4.82 ± 0.31	116.7 ± 6.7	4.28 ± 0.05	119.2 ± 0.3
359[b]	14.55	2.82 ± 0.89	103.8 ± 9.0	4.10 ± 0.30	117.4 ± 1.6	3.76 ± 0.15	122.6 ± 1.1
360[b]	14.52	3.14 ± 0.41	121.3 ± 3.6	3.10 ± 0.09	123.2 ± 0.8	3.31 ± 0.45	123.2 ± 3.8
362[b]	14.48	4.66 ± 0.25	121.4 ± 2.8	5.46 ± 0.27	119.7 ± 0.9	4.70 ± 0.02	117.2 ± 0.1
363[b]	14.61	4.77 ± 0.41	101.8 ± 14.8	5.77 ± 0.27	118.0 ± 1.3	4.60 ± 0.30	119.7 ± 2.1
365[b]	14.56	4.41 ± 0.21	120.8 ± 1.3	4.33 ± 0.04	116.2 ± 0.2	3.88 ± 0.64	120.8 ± 6.3
424[b]	14.41	4.61 ± 0.68	122.7 ± 4.3	4.57 ± 0.02	124.9 ± 0.1	4.46 ± 0.02	116.4 ± 0.1
426[b]	15.11	6.12 ± 1.02	121.8 ± 4.1	5.36 ± 0.22	119.7 ± 1.1	5.12 ± 0.12	120.8 ± 1.1
429[b]	14.92	5.19 ± 0.94	120.8 ± 5.2	4.82 ± 0.14	113.6 ± 1.0	4.96 ± 0.16	121.4 ± 2.5
470[b]	14.03	5.12 ± 0.31	117.4 ± 1.7	4.69 ± 0.05	115.1 ± 0.3	4.20 ± 0.02	118.4 ± 0.1
480[b]	15.47	7.84 ± 1.52	116.9 ± 8.9	6.56 ± 0.93	123.0 ± 4.0	6.78 ± 0.45	120.7 ± 1.9
541[b]	13.71	4.96 ± 0.70	120.7 ± 5.0	5.54 ± 0.46	119.7 ± 2.3	5.18 ± 0.86	120.6 ± 4.7
552[b]	14.47	7.39 ± 0.05	110.1 ± 0.2	7.28 ± 0.13	113.6 ± 4.4	6.86 ± 0.58	118.9 ± 2.4

[a]Common with Guetter & Vrba (1989).
[b]Non-member.

3 RESULTS

Table 2 lists, for the 51 observed stars in the direction of IC 1805, the percentage of polarization, the position angle of the plane of polarization in the equatorial coordinate system and their respective errors for each filters. Membership probabilities, star identification numbers (Id) for all observed stars are taken from Sanders (1972) and the visual magnitude M_V is taken from the work of Joshi & Sagar (1983) and Massey, Johnson & Degioia-Eastwood (1995). The stars with membership probability greater than 50 per cent are considered as the members of IC 1805. Our results for the common stars are in agreement with Guetter & Vrba (1989) within the error limit except P_B. There is a systematic increment of ∼0.45 per cent in P_B measurements for our values from that of Guetter & Vrba (1989).

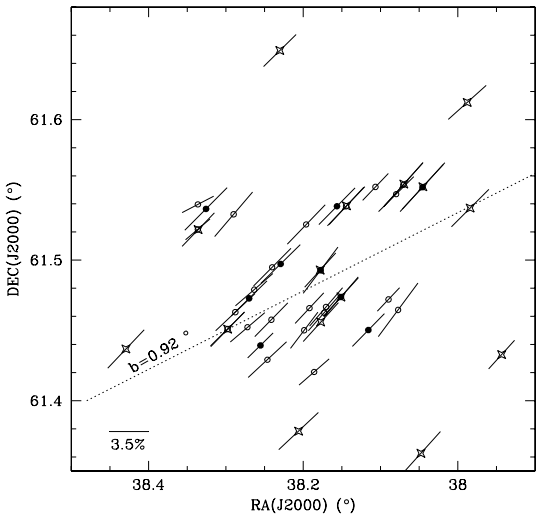

Figure 2. Polarization vectors and their orientations for the stars of IC 1805. The vectors are proportional to the magnitude of the polarization. The scale is indicated in the figure. Filled and open circles indicate members and non-members of cluster IC 1805 observed by us and the starmark indicates the stars observed by Guetter & Vrba (1989). The dotted line is the galactic parallel $b = 0.92^\circ$.

The polarization map for all the stars of IC 1805 observed by us and Guetter & Vrba (1989) is shown in Fig. 2. The length of the polarization vectors is proportional to the degree of polarization (P_V) in per cent (scale is given in the polarization map). The polarization vectors make an angle (θ_V) with the north–south axis (reference axis), which is given in Column 6 of Table 2. The filled and open circles indicate the cluster member and non-member of IC 1805 observed by us, and the starmark indicates the stars observed by Guetter & Vrba (1989). From the polarization map, we can conclude that the alignment of the polarization vectors over the whole observed area are close to being parallel to each other and there is no significant difference between the alignment of the star observed by us and Guetter & Vrba (1989). The alignment of member and non-member stars of cluster IC 1805 is also closely parallel to each other. The orientation of the polarization vectors for the observed stars of IC 1805 indicate that the magnetic field in the direction of the cluster follow a general trend of the polarization directions in the region. The polarization in the cluster has an average direction of $\overline{\theta}_V = 119.96 \pm 0.05$ in equatorial coordinate system. The dotted line superimposed on the Fig. 2 is the galactic parallel $b = 0.92^\circ$ showing a close alignment of the polarization vectors with the projection of the Galactic plane.

4 DUST PROPERTIES

The wavelength (λ_{max}) at which maximum polarization (P_{max}) occurs is a function of the optical properties and characteristic of particle size distribution of the aligned dust grains (McMillan 1978; Wilking et al. 1980). Moreover, it is also related to the interstellar extinction law (Serkowski, Mathewson & Ford 1975; Whittet & van Breda 1978; Coyne & Magalhaes 1979; Clayton & Cardelli 1988). The maximum wavelength λ_{max} and polarization P_{max} have been calculated by fitting the observed polarization in the *BVR* band-passes to the standard Serkowski's polarization law

$$P_\lambda / P_{max} = \exp\left[-k\, ln^2\,(\lambda_{max}/\lambda)\right] \quad (5)$$

Table 3. Polarization results for IC 1805 stars.

Id	$P_{max} \pm \epsilon$ (per cent)	σ_1	$\lambda_{max} \pm \epsilon$ (μm)	$E\,(B-V)$
112[a]	6.76 ± 0.04	0.66	0.54 ± 0.01	0.82
118	5.92 ± 0.02	2.96	0.57 ± 0.01	0.85
121	6.38 ± 0.01	0.05	0.52 ± 0.01	0.88
122	5.20 ± 0.08	0.25	0.55 ± 0.02	–
123	3.32 ± 0.33	3.40	0.58 ± 0.13	0.79
128	3.85 ± 0.05	0.68	0.60 ± 0.02	0.97
129[a]	5.58 ± 0.20	2.00	0.56 ± 0.06	0.81
130[b]	5.54 ± 0.09	2.21	0.51 ± 0.02	–
133[b]	3.59 ± 0.08	0.50	0.56 ± 0.05	–
136	5.58 ± 0.10	2.23	0.55 ± 0.02	0.89
138[a]	6.26 ± 0.18	2.06	0.56 ± 0.04	0.79
139[a]	5.35 ± 0.01	0.31	0.54 ± 0.01	0.76
143	5.10 ± 0.15	4.15	0.57 ± 0.04	0.86
146[b]	5.69 ± 0.27	0.70	0.47 ± 0.03	–
147	4.82 ± 0.07	0.68	0.59 ± 0.03	0.78
149[a]	4.75 ± 0.10	2.33	0.56 ± 0.03	0.70
154	4.30 ± 0.03	0.13	0.53 ± 0.01	0.96
155[b]	4.60 ± 0.16	0.90	0.53 ± 0.04	–
156	4.29 ± 0.08	2.41	0.50 ± 0.03	0.88
157	5.65 ± 0.01	0.13	0.58 ± 0.01	0.89
158	4.38 ± 0.06	1.45	0.57 ± 0.02	1.24
160	5.73 ± 0.06	0.48	0.51 ± 0.01	1.02
162[a]	5.78 ± 0.13	0.36	0.54 ± 0.02	0.67
165	5.50 ± 0.10	1.31	0.53 ± 0.02	0.86
166	4.90 ± 0.09	0.51	0.50 ± 0.02	0.75
168	5.57 ± 0.37	1.04	0.51 ± 0.06	0.96
170[a]	3.73 ± 0.04	0.63	0.55 ± 0.01	0.35
171	5.36 ± 0.07	0.96	0.54 ± 0.01	0.76
173[b]	2.70 ± 0.06	1.11	0.53 ± 0.04	–
174[a]	5.27 ± 0.03	1.73	0.54 ± 0.01	0.75
175	4.92 ± 0.12	0.53	0.50 ± 0.02	0.85
182	5.85 ± 0.03	1.15	0.53 ± 0.01	0.81
183	5.02 ± 0.05	1.40	0.56 ± 0.03	0.88
184[b]	3.96 ± 0.22	1.82	0.51 ± 0.08	–
185[b]	5.61 ± 0.01	0.25	0.48 ± 0.01	–
188[a]	5.26 ± 0.15	2.19	0.54 ± 0.05	0.78
191	4.19 ± 0.05	0.77	0.54 ± 0.02	0.88
192	3.52 ± 0.01	0.11	0.53 ± 0.01	0.76
354[b]	4.84 ± 0.09	0.34	0.48 ± 0.01	–
359[b]	3.90 ± 0.26	1.15	0.56 ± 0.11	–
360[b]	3.12 ± 0.08	0.86	0.55 ± 0.10	–
362[b]	5.01 ± 0.26	1.88	0.52 ± 0.05	–
363[b]	5.36 ± 0.53	2.33	0.50 ± 0.12	–
365[b]	4.44 ± 0.01	0.06	0.47 ± 0.01	–
424[b]	4.58 ± 0.01	0.54	0.57 ± 0.01	–
426[b]	5.47 ± 0.24	0.89	0.52 ± 0.05	–
429[b]	4.95 ± 0.12	1.01	0.62 ± 0.06	–
470[b]	4.88 ± 0.08	0.85	0.46 ± 0.01	–
480[b]	7.24 ± 0.70	0.87	0.51 ± 0.09	–
541[b]	5.46 ± 0.11	0.29	0.57 ± 0.04	–
552[b]	7.45 ± 0.02	0.41	0.48 ± 0.01	–

[a]Frontside stars.
[b]Non-member.

and adopting the parameter $k = 1.15$ (Serkowski 1973). If the polarization is well represented by the Serkowski relation, σ_1 (the unit weight error of the fit) should not be higher than 1.6 due to the weighting scheme; a higher value could be indicative of the presence of intrinsic polarization. In fitting the degree of freedom is adopted as one. Though there are only three data points, the wavelength convey ranges from 0.44 to 0.66 m and all the λ_{max} found to fall within this range.

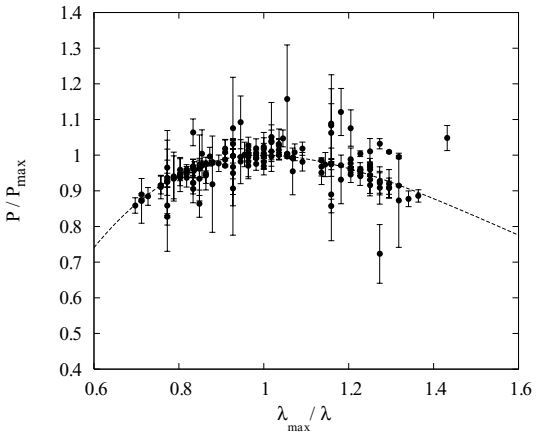

Figure 3. Plot of normalized polarization-wavelength dependence for the observed stars in IC 1805 determined from data listed in Tables 2 and 3. The error bars represent the uncertainties for the measurements of $P/P_{\max}$ and the solid curve denotes the Serkowski polarization relation for general ISM (equation 5).

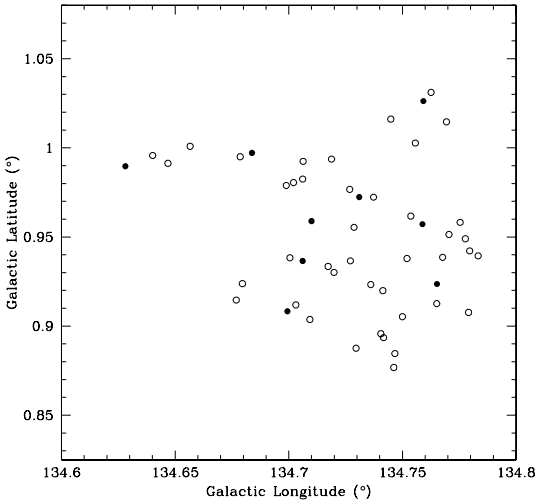

Figure 4. Galactic distribution for all observed stars of IC 1805. Filled circles indicate the *frontside* stars.

Table 3 represents $P_{\max}$, $\lambda_{\max}$ and σ_1 for all the 51 stars with their respective errors. The colour excess $E\,(B-V)$ for different observed stars is taken from the work of Joshi & Sagar (1983). Of the 51 stars observed, 14 of them have the unit weight error of the fit above the limiting value of 1.6 (member stars 174, 156, 143, 149, 138, 129, 123, 188, 136, 118 and non-member stars 363, 362, 130, 184). As mentioned above, the higher value of σ_1 gives a clue about the presence of intrinsic polarization in the light from the star. Therefore, in principle, in the case of IC 1805, interstellar dust alone does not appear to be responsible for the observed polarization. There is also an indication of intrinsic polarization in measurements for some of the observed stars.

The observed normalized polarization-wavelength dependence of the stars in IC 1805 is shown in Fig. 3. The solid curve denotes the Serkowski polarization relation for the general interstellar medium (ISM). In this plot, there exists a good agreement between theory and observations, which indicates that the observed polarization for the stars of IC 1805 is mainly due to the Davis–Greenstein mechanism (Davis & Greenstein 1951) that operates in the general ISM.

The foreground reddening towards IC 1805 is ~ 0.8 mag and the reddening law is anomalous in this direction (Borgman 1961; Johnson 1968; Ishida 1969; Turner 1976). In the direction of IC 1805, the interstellar reddening increases quite linearly up to 1 kpc with an average absorption of about 0.6 mag kpc^{-1}. This indicates that the distribution of interstellar material in the local arm is rather uniform. To remove the effect of interstellar dust located in front of IC 1805 or to determine the effect of intracluster dust on the members of IC 1805, we follow the method described by Marraco et al. (1993). In order to do the same, we have selected a group of nine stars among the members of IC 1805, covering the whole observed region and which seems to be least affected by the reddening. These stars hereafter referred to as *frontside* stars, which are indicated by *a* in Table 3. The *frontside* stars will be used to model the contribution of foreground excess, polarization and finally which will be removed from the remaining member stars to determine the intracluster parameters, respectively.

Fig. 4 shows the Galactic distribution (*l, b*) of all the observed stars in IC 1805. We have used open circles for all the observed stars and filled circles for the selected *frontside* stars. Figs 5(a) and (b) show the colour excess $E\,(B-V)$ plotted as a function of galactic longitude (l) and latitude (b), respectively, filled circles for the selected *frontside* stars and open circles for the other members.

In order to model the effect of foreground extinction, we fit the colour excesses $E\,(B-V)$ for the all nine *frontside* stars to a plane (l, b). The final equation of the fit is

$$E(B-V)(l,b) = 0.088\,6975l + 0.090\,5122b - 11.2302 \text{ (mag)} \quad (6)$$

with an rms error of the unit weight of 0.05. The variation of the excesses with galactic longitude (l) is the most significant part of Marraco's model (Marraco et al. 1993). The observed, modelled and intracluster values of the colour excesses for the non-frontside stars are listed in Table 4. It can be mentioned that the modelled value of the frontside excess led to very small values of the intracluster excess.

The weighted mean of $\lambda_{\max}$ for nine *frontside* stars is

$$\overline{\lambda_{\max}} = 0.544 \pm 0.005\,(\mu\text{m}). \quad (7)$$

This value is quite similar to Guetter & Vrba (1989) for the cluster IC 1805 ($0.54 \pm 0.01\ \mu$m). Moreover, this value does not differ more from the intracluster value of $\lambda_{\max}(0.541 \pm 0.003\ \mu$m). These values are very close to the mean interstellar value of $\lambda_{\max}0.56 \pm 0.04\ \mu$m (Serkowski et al. 1975). Therefore, we can conclude that the characteristic particle size distribution as indicated by the polarization study of stars in IC 1805 is essentially the same as that for the general ISM.

In the case of polarization, the weighted mean of maximum polarization $P_{\max}$ for nine *frontside* stars is

$$\overline{P_{\max}} = 4.865 \pm 0.022 \ \text{(per cent)} \quad (8)$$

and the weighted mean of maximum polarization $P_{\max}$ for the cluster member is 5.008 ± 0.005 (per cent). Therefore, there is also no vast difference between *frontside* and intracluster polarization, the contribution of the intracluster material on polarization is $\simeq$3 per cent. The weighted mean of the polarization position angle $\theta_{\rm V}$ for nine *frontside* is 120.00 ± 0.06. It is possible to calculate $\overline{u}$ and $\overline{q}$, the mean value of normalized Stokes parameters for the group of nine *frontside* stars. Subtracting this mean value from individual u and q for the rest of the observed members of IC 1805 and inverting the procedure, we obtained the values of $P_{\max}$ for intracluster medium and list them in Table 4.

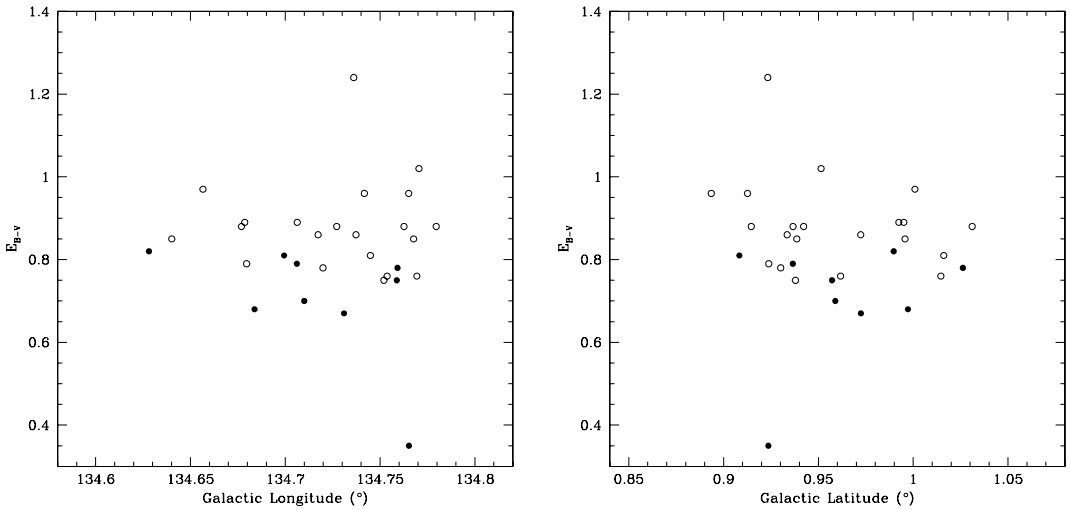

Figure 5. Left-hand panel (a): colour excess $E(B-V)$ plotted as a function of galactic longitude (l). Right-hand panel (b): colour excess $E(B-V)$ plotted as a function of galactic latitude (b). Excesses are taken from Joshi & Sagar (1983). Open circles indicate the observed member stars, and filled circles indicate the *frontside* stars.

Table 4. *BVR* polarization results.

Id	$P_{\max}$ o	$P_{\max}$ f	$P_{\max}$ i	$E\,(B-V)$ o	$E\,(B-V)$ f	$E\,(B-V)$ i
118	5.92	4.82	1.10	0.85	0.72	0.13
121	6.38	4.38	2.00	0.88	0.72	0.16
122	5.20	4.77	0.43	–	0.72	–
123	3.32	1.78	1.54	0.79	0.72	0.07
128	3.85	2.84	1.01	0.97	0.72	0.25
136	5.58	4.86	0.72	0.89	0.72	0.17
143	5.09	4.60	0.49	0.86	0.72	0.14
147	4.82	4.46	0.36	0.78	0.72	0.06
154	4.29	3.39	0.90	0.96	0.72	0.24
156	4.29	3.71	0.58	0.88	0.72	0.16
157	5.65	4.86	0.79	0.89	0.73	0.16
158	4.38	3.29	1.09	1.24	0.72	0.52
160	5.73	4.75	0.98	1.02	0.73	0.29
165	5.53	4.84	0.69	0.86	0.73	0.13
166	4.90	4.76	0.14	0.75	0.73	0.02
168	5.57	4.69	0.88	0.96	0.72	0.24
171	5.37	4.41	0.97	0.76	0.73	0.03
175	4.92	4.08	0.84	0.85	0.73	0.12
182	5.85	4.72	1.13	0.81	0.73	0.08
183	5.03	4.72	0.31	0.88	0.73	0.15
191	4.24	2.31	1.93	0.88	0.73	0.15
192	3.51	1.98	1.53	0.76	0.73	0.03

$P_{\max}$ in per cent and $E(B-V)$ in mag.
o: Observed.
f: Foreground.
i: Intracluster.

In diffused ISM, the polarization efficiency (ratio of the maximum amount of polarization to visual extinction) cannot exceed the empirical upper limit

$$P_{\max} < 3A_{\rm V} \simeq 3R_{\rm V} \times E(B-V) \qquad (9)$$

which is obtained for interstellar dust particles (Hiltner 1956). The ratio $P_{\max}/E\,(B-V)$ mainly depends on the alignment efficiency, magnetic strength and also the amount of depolarization due to radiation traversing more than one cloud with different direction. Fig. 6 shows the relation between $P_{\max}$ and colour excess $E\,(B-V)$ for the members and *frontside* stars of IC 1805. Except the *frontside* star-170, no star lies at the left block of the interstellar maximum line. Though, the *frontside* star-170 falls at the left block of the interstellar maximum line, but the value of σ_1 for the star-170 is 0.63 [unit weight error of fitting of Serkowski polarization relation (equation 5)], which is much below than the limiting value 1.6. Therefore, there is very less possibility of having intrinsic polarization in star-170. The polarization efficiency plot for the members of IC 1805 indicates that apparently the stars are not affected by intrinsic polarization. The dominant mechanism of polarization in the observed section of IC 1805 is supposed to be the alignment of grains by magnetic field in a similar way as that found in the general ISM.

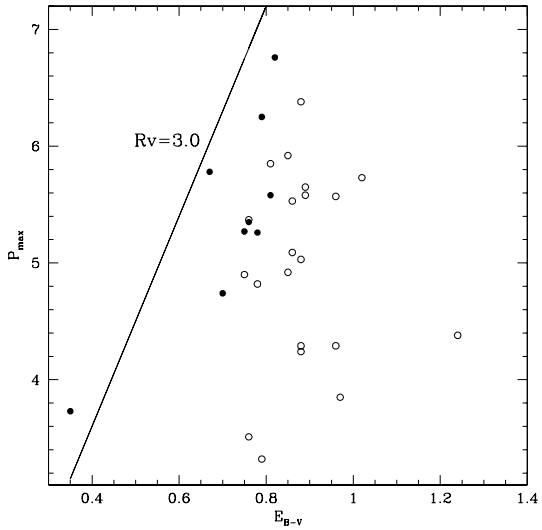

Figure 6. Polarization efficiency diagram for the observed dust. Using $R_{\rm V} = 3.0$, the line of maximum efficiency drawn. Filled and open circles indicate *frontside* and *non-frontside* members of IC 1805.

5 CONCLUSIONS

The main results of the *BVR* polarimetric study of IC 1805 can be summarized as follows.

The mean value of maximum polarization $P_{\max}$ of IC 1805 for foreground is 4.865 ± 0.022 per cent and while for the intracluster medium is 5.008 ± 0.005 per cent. The contribution of the intracluster dust on polarization is $\simeq$3 per cent.

The mean wavelength dependence of polarization $\lambda_{\max}$ for the cluster member is $0.541 \pm 0.003\,\mu$m and for foreground is $0.544 \pm 0.005\,\mu$m. The very less dispersion of $\lambda_{\max}$ indicates that the mean intracluster grain size is quite similar to general ISM.

Though the observed polarization of some of the stars in IC 1805 may be due to intrinsic stellar polarization in their measurements, but the dominant mechanism is polarization due to the general ISM. The difference between foreground and intracluster colour excess is negligible in the direction of IC 1805. There is very little evidence of dust in the intracluster region. The highly polarized and reddened stars may be projected through various discrete foreground clouds, which have different grain sizes and compositions.

ACKNOWLEDGMENTS

This research has made use of the WEBDA data base, operated at the Institute for Astronomy of the University of Vienna, use of image from the National Science Foundation and Digital Sky Survey (DSS), which was produced at the Space Telescope Science Institute under the US Government grant NAG W-2166, use of NASA's Astrophysics Data System and use of IRAF, distributed by National Optical Astronomy Observatories, USA. We thank the referee for his constructive comments which have lead to a considerable improvement in the paper. BJM would like to thank Orchid, Amitava, Manash, Sanjeev and Jessy for their support.

REFERENCES

Borgman J., 1961, Bull. Astron. Inst. Neth., 16, 99
Clayton G. C., Cardelli J. A., 1988, AJ, 96, 695
Coyne G. V., Magalhaes A. M., 1979, AJ, 84, 1200
Davis L., Jr, Greenstein J. L., 1951, ApJ, 114, 206
Guetter H. H., Vrba F. J., 1989, AJ, 98, 611
Hiltner W. A., 1956, ApJS, 2, 389
Ishida K., 1969, MNRAS, 144, 55
Johnson H. L., 1968, in Middlehurst B. M., Aller L. H., eds, Nebulae and Interstellar Matter. Univ. Chicago Press, Chicago, p. 167
Joshi U. C., Sagar R., 1983, J. R. Astron. Soc. Can., 77, 40
Marraco H. G., Vega E. I., Vrba F. J., 1993, AJ, 105, 258
Massey P., Johnson K. E., Degioia-Eastwood K., 1995, ApJ, 454, 151
McMillan R. S., 1978, ApJ, 225, 880
Ramaprakash A. N., Gupta R., Sen A. K., Tandon S. N., 1998, A&AS, 128, 369
Rautela B. S., Joshi G. C., Pandey J. C., 2004, Bull. Astron. Soc. India, 32, 159
Sagar R., 1987, MNRAS, 228, 483
Sagar R., Yu Q. Z., 1990, ApJ, 353, 174
Sanders W. L., 1971, A&A, 14, 226
Sanders W. L., 1972, A&A, 16, 58
Schmidt G. D., Elston R., Lupie O. L., 1992, AJ, 104, 1563
Serkowski K., 1973, Int. Astron. Union Symp., 52, 145
Serkowski K., Mathewson D. L., Ford V. L., 1975, ApJ, 196, 261
Shi H. M., Hu J. Y., 1999, A&AS, 136, 313
Tinbergen J., 1996, Introduction to Astronomical Polarimetry. Cambridge Univ. Press, Cambridge
Turner D. G., 1976, AJ, 81, 1125
Vasilevskis S., Sanders W. L., van Altena W. F., 1965, AJ, 70, 806
Whittet D. C. B., van Breda I. G., 1978, A&A, 66, 57
Wilking B. A., Lebofsky M. J., Kemp J. C., Martin P. G., Rieke G. H., 1980, ApJ, 235, 905

This paper has been typeset from a TEX/LATEX file prepared by the author.